Vertically integrated thin-film color sensor arrays for advanced sensing applications

H. Steibig
Research Center Jülich, Institute of Photovoltaics, 52425 Jülich, Germany

R. A. Street and D. Knipp[a)]
Palo Alto Research Center, Electronic Materials Laboratory, Palo Alto, California 94304

M. Krause[b)]
Research Center Jülich, Institute of Photovoltaics, 52425 Jülich, Germany

J. Ho
Palo Alto Research Center, Electronic Materials Laboratory, Palo Alto, California 94304

(Received 24 May 2005; accepted 27 October 2005; published online 5 January 2006)

A three-color sensor array based on a vertically integrated thin-film structure is reported. The complete color information can be detected at the same position of a sensor array without using optical filters. The sensors consist of a multilayer thin-film system utilizing amorphous silicon and its alloys. The spectral sensitivity of the sensors is controlled by the optical properties of the materials and the applied bias voltage. The color sensors were integrated with amorphous silicon readout electronics to realize a large area thin-film three color sensor array. The working principle of the thin-film sensor arrays is presented with a discussion of the spectral sensitivity and the pixel cross talk. © *2006 American Institute of Physics*. [DOI: 10.1063/1.2140072]

Optical sensing is usually performed by silicon sensor arrays in combination with color filter arrays (CFAs). The color filter array is typically realized by a spatial arrangement of at least three types of optical filters for the colors red, green, and blue. Therefore, three chromatic color pixels are required to form a color pixel, which limits the resolution of conventional sensor arrays. Furthermore, color detection using CFAs may lead to color moiré or color aliasing effects, which are observed when structures with high spatial frequencies are taken.

In order to overcome the color moiré effect, vertically integrated sensor structures have been proposed, which detect the color information in the depth of the sensor structure. Due to the wavelength dependent absorption of the semiconductor material, the color information can be detected as a function of the penetration depth of the photons in the material. Various two- or three-color sensor structures have been realized by using different materials, design concepts, and contact configurations.[1–10] The suggested sensors range from two-terminal devices, which change their spectral sensitivity by varying the applied bias voltage to vertically stacked diodes. Even though the color moiré effect is more pronounced for larger pixels, vertically integrated three-color sensors in combination with large area electronics have not been demonstrated.

Large-area sensor arrays are of interest for a variety of applications, where the requirements of cost and scalability are different from classical silicon microelectronics. Typical examples are lab-on-chip systems using microfluidics in combination with optical or electronic readout circuitry. For instance, the dimensions of microfluidic channels are limited by surface tension, which prevents scaling down of the structures to the submicrometer range.

The sensor arrays were fabricated by plasma-enhanced chemical vapor deposition at temperatures below 300 °C on 4 in. glass wafers. A cross section of a sensor pixel of the sensor array is shown in Fig. 1. The optical sensor is integrated on top of a readout backplane to achieve a high area fill factor. The sensor array has a resolution of 512 $\times$512 pixels and a pixel pitch of 100 μm$\times$100 μm. Pixel addressing is realized by amorphous-silicon thin-film transistors (TFTs). Each pixel contains a bottom gate TFT, a storage capacitor, address and data lines, and a contact pad to the sensor occupying 67% of the pixel area. A detailed description of the deposition parameters and the device performance of the amorphous-silicon TFT is given elsewhere.[11]

The color sensor is realized by the back-to-back connection of two amorphous-silicon *p-i-n* diodes. The band diagram of the optical sensor under thermal equilibrium is shown in Fig. 2. Only the back contact and the *n* layer of the bottom diode were patterned. The remaining layers of the optical sensor and the top electrode of the sensor array were unpatterned. The top contact of the sensor array was realized

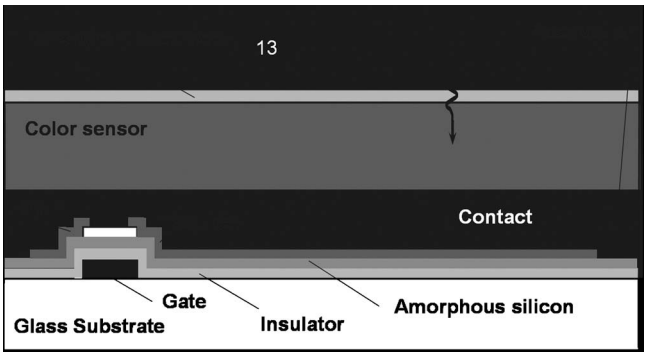

FIG. 1. Cross section of a pixel of a large-area color sensor array.

[a)]Also at: International University Bremen, Department of Science and Engineering, 28759 Bremen, Germany; electronic mail: d.knipp@iu-bremen.de
[b)]Present address: Infineon Technology, Dresden, Germany.

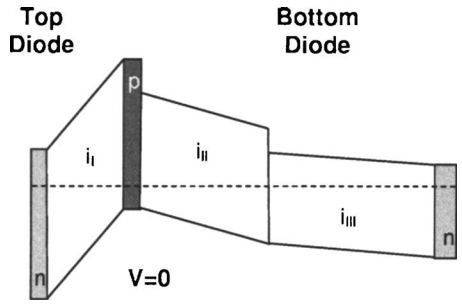

FIG. 2. Schematic band structure of a *n-i-p-i-n* color sensor under thermal equilibrium.

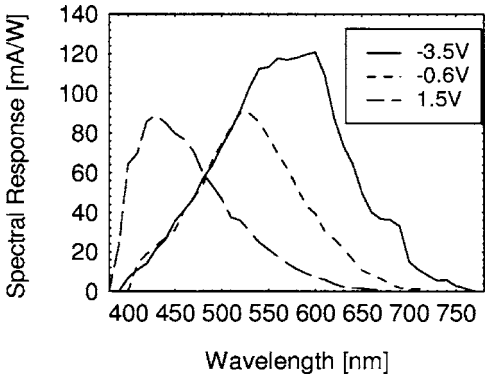

FIG. 3. Spectral response of the *n-i-p-i-n* sensors for the applied bias voltages of $V=+1.5$ V, −0.6 V, and −3.5 V.

by radio-frequency magnetron sputtered ZnO.[12]

To minimize the color error of the sensor, the spectral sensitivity of the detector has to be matched to the color space of the human eye. Thus, band-gap engineering of the individual regions of the sensor is needed to optimize the spectral sensitivities. The top diode (the diode which is first penetrated by the incoming light) of the sensor is realized by a diode with an amorphous-silicon–carbon alloy absorber. The absorber in the top diode (i_I layer) has an optical band gap of 2.2 eV and a thickness of 85 nm. Therefore, blue light is absorbed in the top diode, whereas green and red light is transmitted through the top diode. The absorber of the bottom diode is divided in two regions consisting of a silicon carbon layer with an optical band gap of 1.9 eV (Region i_{II}) and an intrinsic amorphous silicon layer with an optical band gap of 1.74 eV (Region i_{III}). A detailed description of the deposition conditions of the materials is given elsewhere.[13] To facilitate the separation of two different colors within a single diode, a very thin lightly *n*-type-doped layer was introduced between the two absorption layers of the bottom diode. The thin lightly doped layer leads to an increased electric field in Region i_{II} which has a thickness of 145 nm, whereas the electric field in region i_{III} with a thickness of 365 nm is reduced.

The spectral sensitivity of the device is controlled by the bias voltage that is applied to the sensor. Applying a positive voltage to the *n-i-p-i-n* sensor leads to a reverse biased top diode and a forward biased bottom diode. Under this condition, the photogenerated carriers in the top diode determine the overall photocurrent, whereas the photogenerated carriers in the bottom diode recombine. Therefore, the detector yields blue sensitivity. Changing the applied bias to a negative voltage leads to a forward biased top diode and a reverse biased bottom diode. In this case, the sensor is green or green and red sensitive. For low negative voltages, the electric field in Region i_{II} is much higher than the electric field in Region i_{III}, so that the photogenerated carriers in region i_{II} determine the photocurrent. For higher negative voltages, the electric field is enhanced throughout the entire bottom diode, and the extracted carriers out of Regions i_{II} and i_{III} determine the photocurrent.

The spectral response of a *n-i-p-i-n* sensor integrated on top of the TFT backplane is shown in Fig. 3. For a bias voltage of +1.5 V, the sensor exhibits a maximum of the spectral sensitivity at a wavelength of 430 nm. Applying a negative bias to the optical sensor leads to the extraction of carriers out of the bottom diode. For low negative voltages of −0.6 V, the sensor exhibits green sensitivity. The sensor exhibits a maximum of the spectral sensitivity at 530 nm. For higher negative bias almost all carriers can be extracted out of Regions i_{II} and i_{III}, and the maximum of the spectral response shifts to 600 nm.

A color image taken by the thin-film sensor array is shown in Fig. 4. The image with a resolution of 185 $\times$ 280 pixels consists of three images captured for the applied bias voltages of −3.5 V (red and green), −0.6 V (green), and 1.5 V (blue). An integration time of 50 ms was used to acquire the images. The image taken for −3.5 V was corrected to get a red signal before merging the red, green, and blue images. No further colorimetric transformation of the signals were carried out to improve the color error.

The spatial resolution of the red-green-blue image is limited by the blue image. This is caused by the fact that only the *n* layer of the bottom diode and the back contact of the sensor were patterned. The remaining layers, including the top diode, were unpatterned. As a consequence, the spatial resolution of images taken by the top diode is reduced and

FIG. 4. (Color online) Color image taken by a moiré free large-area color senor array. The image has a resolution of 185 $\times$ 280 pixels.

pixel cross talk is observed, particularly at defects in the backplane. These results are confirmed by measurements of the line spread function and the modulation transfer function. The increased cross talk is caused by an electric-field gradient in the *p* layer of the sensor. Different levels of light intensity lead to different potentials in the *p* layer. Therefore, a spatial variation of the light intensity leads to an electric-field gradient along the *p* layer, which causes charge to flow between pixels, resulting in cross talk.

In summary, for the first time, a three-color large-area sensor array free of moiré effect or color aliasing is presented. The sensor array was realized on glass substrates with a resolution of 512×512 pixels. Amorphous-silicon and its alloys were deposited at temperatures below 300 °C to realize the optical sensor and the readout transistors of the sensor array. Due to the vertical integration of the sensor channels, the complete color information can be detected at the same position of a sensor array without the aid of optical filters. The color detector based on the antiserial connection of two amorphous diodes. Top and bottom diodes exhibit a good color separation and a high dynamic range. The large-area sensor arrays are of particular interest for applications where the requirements in terms of cost and scalability are different from classical microelectronics. Such applications are, for instance, lab-on-chip systems.

The authors would like to thank the research groups of B. Rech and F. Finger for their assistance in preparing the color sensor and the team of the process line at the Palo Alto Research Center for fabricating the TFT backplane.

[1] R. F. Lyon and P. M. Hubel, in *Proceedings of the IS&T/SID Color Imaging Conference* (2002), p. 349.
[2] P. Seitz, D. Leipold, J. Kramer, and J. M. Raynor, Proc. SPIE **1900**, 21 (1993).
[3] D. P. Poenar and R. F. Wolfenbuttel, Appl. Opt. **36**, 5109 (1997).
[4] H. K. Tsai and S.-C. Lee, Appl. Phys. Lett. **52**, 275 (1988).
[5] H. Stiebig, J. Giehl, D. Knipp, P. Rieve, and M. Böhm, Mater. Res. Soc. Symp. Proc. **377**, 517 (1995).
[6] J. Zimmer, D. Knipp, H. Stiebig, and H. Wagner, IEEE Trans. Electron Devices **45**, 884 (1999).
[7] P. Rieve, M. Sommer, M. Wagner, K. Seibel, and M. Böhm, J. Non-Cryst. Solids **266**, 1168 (2000).
[8] D. Knipp, H. Stiebig, J. Fölsch, F. Finger, and H. Wagner, J. Appl. Phys. **83**, 1463 (1998).
[9] F. Palma, *Springer Series in Material Science* Vol. 37, edited by R. A. Street (Springer, Berlin, 2000), pp. 306–338.
[10] F. Lemmi, M. Mulato, J. Ho, R. Lau, J. P. Lu, R. A. Street, and F. Palma, Appl. Phys. Lett. **78**, 1334 (2001).
[11] R. A. Street, Springer Series in Material Science Vol. 37, edited by R. A. Street (Springer, Berlin, 2000).
[12] O. Kluth, A. Löffl, S. Wieder, C. Beneking, L. Houben, B. Rech, H. Wagner, S. Waser, J. A. Selvan, and H. Keppner, Proc. IEEE, 715 (1997).
[13] W. Luft and Y. Tuso, *Hydrogenated Amorphous Silicon Alloy Deposition Processes* (Marcel Dekker, New York, 1993).